Roles of Two Conserved Amino Acid Residues in the Active Site of Galactose-1-Phosphate Uridylyltransferase: An Essential Serine and a Nonessential Cysteine†

Sandaruwan Geeganage, Vicky Wai Kee Ling, and Perry A. Frey*

Institute for Enzyme Research, The Graduate School, and Department of Biochemistry, College of Agricultural and Life Sciences, University of Wisconsin—Madison, 1710 University Avenue, Madison, Wisconsin 53705

Received November 9, 1999; Revised Manuscript Received March 3, 2000

ABSTRACT: Galactose-1-phosphate uridylyltransferase (GalT) catalyzes the reversible transformation of uridine 5′-diphosphate glucose (UDPGlc) and galactose-1-phosphate into uridine 5′-diphosphate galactose (UDPGal) and glucose-1-phosphate through a double displacement mechanism, with the intermediate formation of a covalent uridylyl-enzyme (UMP-enzyme). The covalent linkage is a phosphoramidate formed between the UMP moiety and the His 166 $N^{\epsilon 2}$ of GalT, with His 166 $N^{\delta 1}$ retaining a proton throughout the catalytic cycle. Cys 160 and Ser 161 in *Escherichia coli* GalT are engaged in hydrogen bonding with the peripheral phosphoryl oxygen atoms of the substrate in the crystalline UMP-enzyme and in the crystalline complex of H166G-GalT with UDPGlc [Wedekind, J. E., Frey, P. A., and Rayment, I. (1996) *Biochemistry 35*, 11560−11569; Thoden, J. B., Ruzicka, F. J., Frey, P. A., Rayment, I., and Holden, H. M. (1997) *Biochemistry 36*, 1212−1222]. Site-directed mutagenesis, thermodynamic, transient kinetic, and steady-state kinetic studies have been performed to investigate the roles of Cys 160 and Ser 161 in catalysis. The absence of the thiol group of Cys 160 in the variants C160S and C160A did not seriously alter the enzymatic activity. However, the variant S161A displayed 7000-fold less activity than wild-type GalT. The low activity of S161A was directly related to impaired uridylylation rate constant (3.7×10^{-2} s^{-1}) and de-uridylylation rate constant (0.5×10^{-2} s^{-1}) resulting from a higher kinetic barrier for uridylyl-group transfer by the variant S161A as compared with the wild-type GalT. Equilibrium uridylylation studies showed that neither Cys 160 nor Ser 161 was involved in stabilizing the uridylyl-enzyme intermediate. The results lead to the conclusion that the conserved Cys 160 does not play a critical role in catalysis. Ser 161 is most likely involved in donating a hydrogen bond to the β-phosphoryl group of a substrate, thereby providing proper orientation for nucleophilic catalysis.

GalT[1] (galactose-1-phosphate uridylyltransferase, EC 2.7.7.12) is an enzyme of the Leloir pathway of galactose metabolism (Scheme 1) (*1*). It catalyzes the nucleotide exchange between uridine 5′-diphosphate glucose (UDPGlc) and galactose-1-phosphate (Gal-1-P) to produce uridine 5′-diphosphate galactose (UDPGal) and glucose-1-phosphate (Glc-1-P) by a ping-pong kinetic mechanism, in which His 166 serves as the nucleophilic catalyst.

GalT plays a major role in galactose metabolism, in which galactose is converted into Glc-1-P. It also provides the means for equilibrating uridylylated sugars in the cell (*2*). The UDP-hexoses are needed in the synthesis of disaccharides, glycoproteins, glycolipids, and cellulose (*1*). The human autosomal recessive genetic disease galactosemia results from the impairment of GalT activity, leading to high levels of galactose and Gal-1-P (*3*). The symptoms include cataracts, jaundice, cirrhosis, brain damage, and neurodevelopmental problems (*4*). These symptoms can be alleviated by placing patients on a galactose-restricted diet, but a number of secondary complications such as mental retardation, learning disorders, ovarian cancer, and decreased fertility often develop later in life (*5*−*7*).

Scheme 1

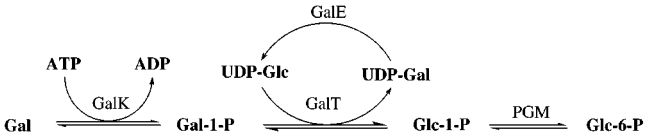

GalT from *Escherichia coli* is a dimer of molecular mass 80 kDa and contains 348 amino acids per subunit (*8*) and ∼1.2 mol of Zn^{2+} and ∼0.7 mol of Fe^{2+}/mol of subunits. The metal ions do not participate in catalysis but are required for enzymatic activity (*8*−*10*). The crystal structure of *E.*

† This research was supported by Grant GM30480 from the National Institute of General Medical Sciences, USPHS.

* To whom correspondence should be addressed. Telephone: (608) 262-0055. Fax: (608) 265-2904. E-mail: frey@biochem.wisc.edu.

[1] Abbreviations: GalT, galactose-1-phosphate uridylyltransferase; PGM, phosphoglucomutase; UDPGlc, uridine 5′-diphosphate glucose; Gal-1-P, galactose-1-phosphate; UDPGal, uridine 5′-diphosphate galactose; Glc, glucose; Glc-1-P, glucose-1-phosphate; NAD^+, nicotinamide adenine dinucleotide; $NADP^+$, nicotinamide adenine dinucleotide phosphate; PMSF, phenylmethanesulfonyl fluoride; bicine, *N*,*N*-bis(2-hydroxyethyl)glycine; HEPES, *N*-(2-hydroxyethyl)piperazine-*N*′-2-ethanesulfonic acid; EDTA, ethylenediaminetetraacetic acid; SDS−PAGE, sodium dodecyl sulfate−polyacrylamide gel electrophoresis; ICP-MS, inductively coupled plasma emission mass spectrometry; *p*-CMB, *p*-chloromercuribenzoic acid.

10.1021/bi992594s CCC: $19.00
Published on Web 04/13/2000

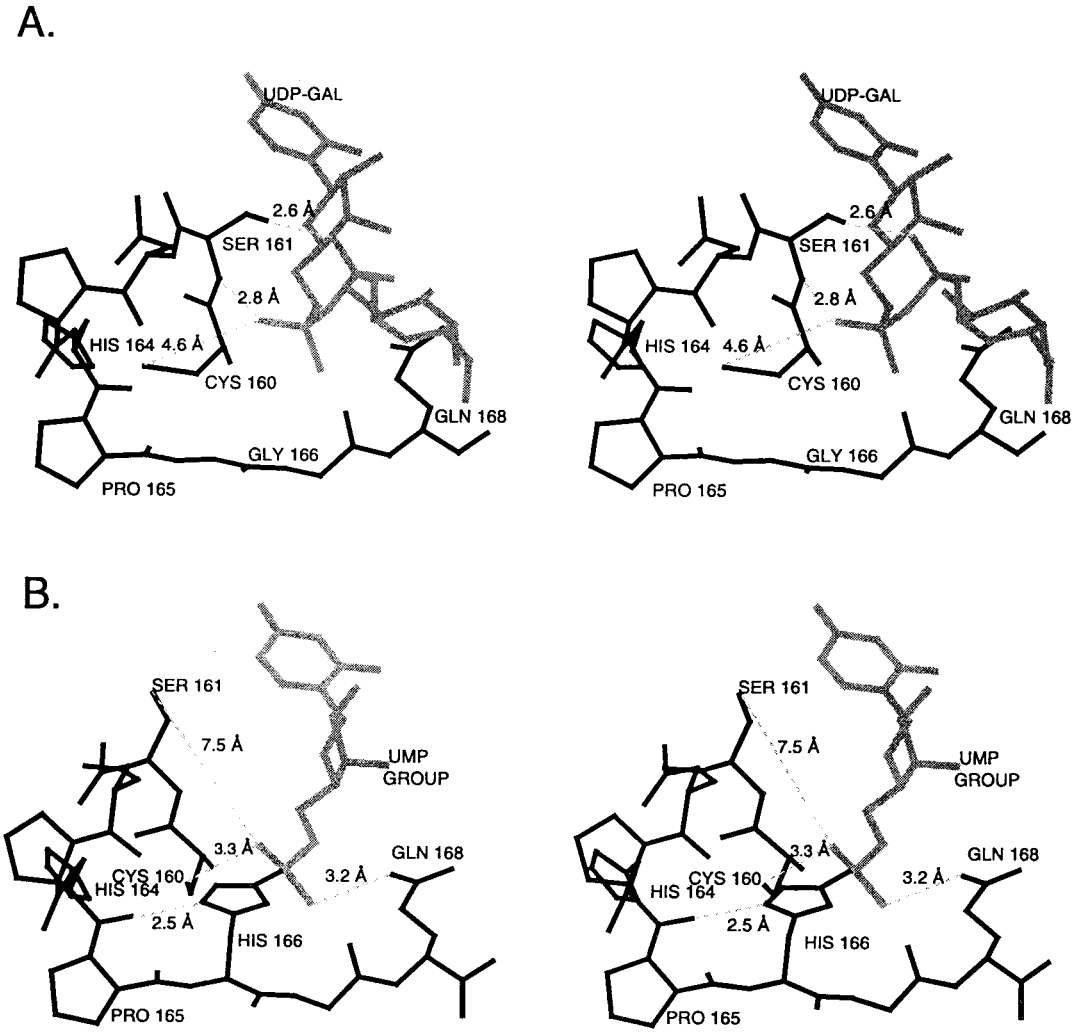

FIGURE 1: Stereoviews of the active sites of UDPGal in complex with H166G-GalT complex and of uridylyl-GalT. (A) Structure of the active site of H166G-GalT in complex with UDPGal (gray) shows the interactions of Gln 168 with phosphoryl oxygens and the interaction of Ser 161 O^{g} with the β-phosphoryl group. Note also that the main chain amide proton of Ser 161 is pointing toward the α-phosphoryl group. The vacant space left by the mutation of H166 to G166 is occupied by a hydrated K^{+} ion (not shown). The side chain of Cys 160 is rotated away from the substrate. The distances between relevant atoms are given in the figure. (B) Structure of the active site of uridylyl-GalT shows the UMP group's (gray) phosphate oxygen interacting with the side chains of Gln 168 and Cys 160 S^{γ}. Ser 161 is rotated away from the substrate in this structure. Note the backbone carbonyl of His 164 2.5 Å away and oriented toward the $N^{\delta 1}$ of His 166. Figures were made from coordinates deposited at the Protein Data Bank (1GUP, UDPGal·H166G-GalT; 1HXQ, uridylyl-GalT) (*12*, *14*). Mol View 1.4.8 was used for generating the figures (*26*).

coli GalT with UDP bound at the active site and the structure of the uridylyl-enzyme intermediate have provided information about residues interacting closely with His 166 and the uridine-5′-phosphoryl group (*11*, *12*). The structure of UDP-hexose synthase, the H166G variant of GalT (*13*), has also been solved with UDPGlc or UDPGal bound to the active site (*14*).

Gln 168, which is conserved in all known GalTs, faces the active site and is near His 166 (Figure 1). In the uridylyl-enzyme structure, Gln 168 interacts closely with phosphoryl oxygen atoms (Figure 1). One of the most common natural mutations associated with human galactosemia is the substitution of arginine for this glutamine (*15*, *16*). Gln 188 in the human enzyme corresponds to Gln 168 in GalT from *E. coli*, the amino acid sequence of which is 56% identical to the human enzyme. We have shown that the *E. coli* Q168R-GalT is less active than the wild-type enzyme by a factor of 10^{5}, and it displays similar impairments in its uridylylation and de-uridylylation rates (*17*).

In the first step of the mechanism, His 166 in the active site of the *E. coli* enzyme attacks the α-phosphorus of UDPGlc, displaces Glc-1-P, and forms the high-energy, covalent uridylyl-enzyme (UMP-enzyme) intermediate (Scheme 2). The uridylyl-enzyme reacts with Gal-1-P in the next step to produce UDPGal. Because the imidazole ring of His 166 in the uridylyl-enzyme remains protonated throughout the catalytic cycle (Scheme 2), and the value of pK_a for the imidazole group in uridine-5′-phosphoimidazolide, a model for the uridylyl-enzyme, is 5.6, the uridylyl-enzyme must be stabilized by noncovalent binding interactions corresponding to ≥ 4.5 kcal mol^{-1} (*18*). The transition-state leading to uridylyl-enzyme formation and reaction must also be significantly stabilized by neutralization of the developing charges on phosphoryl oxygens. Because mutation of Gln 168 to Asn 168, Gly 168, or His 168 affected catalysis only moderately, we searched for other residues that interact with the phosphoryl portion of the substrate and that might stabilize the intermediate and the transition states.

Scheme 2

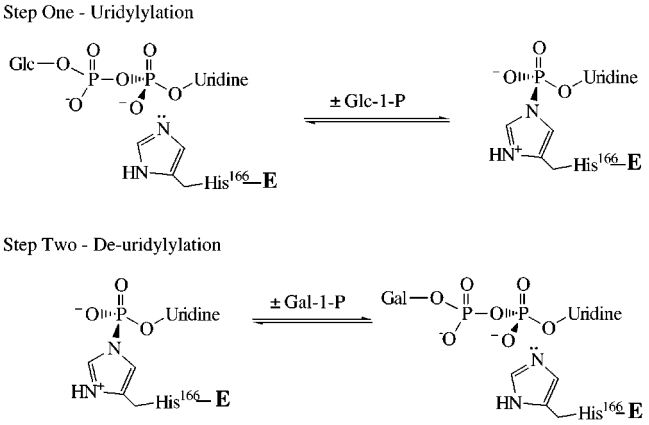

Cys 160 and Ser 161 appeared to contribute the only other groups interacting directly with the phosphoryl oxygen atoms in the three available crystal structures (*11*, *12*, *14*).

In the uridylyl-enzyme, the β-SH of Cys 160 lies at a distance of 3.3 Å from a nonbridging phosphoryl oxygen, and the other nonbridging oxygen is hydrogen bonded to Gln 168. Previous work from this laboratory showed that GalT activity could be eliminated by treatment with cysteine-modifying agents such as *p*-CMB (*19*). Therefore, Cys 160 was a candidate for stabilization of the intermediate and transition states in catalysis. In the structure of H166G-GalT with UDPGlc or UDPGal bound in the active site, Ser 161 interacts with a nonbridging β-phosphoryl oxygen at a distance of 2.6 Å. Interestingly, in the structure of the uridylyl-enzyme, Ser 161 is rotated away from the uridylyl-group to a distance of 7.5 Å from the phosphoryl oxygen atoms. Both Cys 160 and Ser 161 are highly conserved, and their role in the mechanism is of interest. We therefore constructed variants C160S, C160A, and S161A and characterized them kinetically and thermodynamically. The present results and conclusions are presented in this paper.

MATERIALS AND METHODS

Materials. Glc-1-P, Gal-1-P, UDPGlc, NAD^+, NADP, glucose-6-phosphate dehydrogenase, phosphoglucomutase, UDPGlc dehydrogenase, β-mercaptoethanol, PMSF, bicine, and HEPES were from Sigma. Affi-Gel Blue was from Bio-Rad. Amicon membranes and Microcon Concentrators were from Amicon. Q-Sepharose was from Pharmacia. All molecular biology supplies were from Promega and Fisher.

Site-Directed Mutagenesis. Site-directed mutagenesis was performed by using the Bio-Rad Mutagene site-directed mutagenesis kit, which is based on the method of Kunkel (*20*). The *galT* gene has previously been cloned into the high expression vector pTZ18ROT (*21*). All oligonucleotide primers were purchased from Life Technologies. The mutagenic primers were 22 bases long and contained the central coding mutations TGC → GCC for Cys 160 → Ala 160; TGC → TCC for Cys 160 → Ser 160; and TCT → GCT for Ser 161 → Ala 161. The Cys → Ala codon change introduced a *Nar*I site, and the Cys → Ser codon change introduced a *Bam*HI site. Mutant colonies were identified by restriction digestion or by DNA sequencing. The mutated genes were sequenced in their entire length, by ABI Prism Ampli Taq sequencing in the University of Wisconsin—Madison Biotechnology Center to verify the absence of adventitious mutations. Plasmids carrying mutated genes pTZ18ROC160A, pTZ18ROC160S, and pTZ18ROS161A were transformed into BL21(DE3)pLysS cells and overexpressed as described previously (*21*).

Protein Purification. Wild-type GalT was purified as described previously (*22*). The variants C160A- and S161A-GalT were purified by a minor modification of the same procedure. The ammonium sulfate precipitation steps were excluded, and the supernatant fluid from the streptomycin sulfate precipitation was diluted to 4 mg mL^{-1} protein and applied directly to the Affi-Gel Blue affinity column. Fractions from the Q-Sepharose column were pooled, concentrated, and stored in liquid nitrogen. SDS−PAGE analysis indicated that mutated proteins purified under this protocol showed only one band in an overloaded gel upon Coomassie staining and appeared to be more than 95% pure.

Metal Analysis. All metal analyses were performed at the University of Wisconsin—Madison Plant and Soil Analysis Laboratory by ICP-MS. Highly purified GalT was diluted in Nanopure water and submitted for Fe and Zn analysis. Each analysis was complemented by appropriate control experiments. Protein concentrations were measured spectrophotometrically using the extinction coefficient (72 400 M^{-1} cm^{-1}) for GalT at 280 nm (*10*).

Spectroscopy. UV−visible spectrophotometry was performed either on a Hewlett-Packard model 8452A diode array spectrophotometer or on a Shimadzu model 1601PC spectrophotometer. Fluorescence spectra were obtained on a Perkin-Elmer model MPF-3 spectrofluorometer. Circular dichroism spectra were obtained on an Aviv model 62ADS CD spectrometer at the Biophysics Instrumentation Facility of the Department of Biochemistry at the University of Wisconsin—Madison.

Enzymatic Assays. GalT activity was measured by a standard coupled assay (*23*). Assays were carried out in 1-mL cuvettes in sodium bicinate buffer at pH 8.5 in the presence of 10 mM β-mercaptoethanol. The formation of Glc-1-P was coupled to NADPH formation by PGM and Glc-6-phosphate dehydrogenase. The formation of the uridylyl-enzyme was observed and quantified spectrophotometrically under the conditions of the standard assay with the omission of Gal-1-P. Under these conditions, the amount of NADPH formed is equal to the amount of uridylyl-enzyme formed. The uridylyl-enzyme content of GalT was measured and quantified spectrophotometrically by adding Glc-1-P to the uridylyl-enzyme. The UDPGlc formed was coupled to NADH production by UDPGlc dehydrogenase. In this reaction, 2 mol of NADH/mol of UDPGlc are produced.

Steady-state kinetic parameters for C160A- and S161A-GalT at 27 °C were measured using coupled enzyme systems (PGM, Glc-6-P dehydrogenase, forward direction; UDPGlc dehydrogenase, reverse direction) described above. In the forward direction, the rates of formation of Glc-1-P were measured at varying UDPGlc and Gal-1-P concentrations. In the reverse direction, the rates of formation of UDPGlc were measured at varying UDPGal and Glc-1-P concentrations. Necessary control experiments were performed to ensure that GalT limited the observed rates in the assay. Measured rates were normalized for the amount of enzyme added and were computer-fitted to the following equation for the ping-pong kinetic mechanism as described (*24*): v

$= V[A][B]/\{K_a[B] + K_B[A] + [A][B]\}$, where A is either UDPGlc or UDPGal, and B is either Gal-1-P or Glc-1-P. Steady-state kinetic studies for S161A-GalT at 4 °C were performed by using ^{14}C-labeled UDPGlc in a timed point assay as described previously (*17*).

Transient-State Kinetics. Uridylylation and de-uridylylation rates for S161A-GalT at 4 °C were measured as described previously (*17*). The uridylylation rate was measured at 5.1 mM UDPGlc, and the de-uridylylation rate was measured at 5.1 mM Glc-1-P to facilitate comparison with values previously obtained for wild-type GalT.

Free Energy of Uridylylation. Equilibrium constant measurements and free energy calculations were performed as described previously (*22*). Wild-type or mutated forms of GalT were permitted to react with excess UDPGlc to uridylylation equilibrium, quenched by heating with EDTA, and the Glc-1-P produced was measured enzymatically. Uridylylation follows the course of eqs 1−3, where E−UMP represents the uridylyl-enzyme, with the UMP group co-

$$\text{E} + \text{UDPGlc} \rightleftharpoons \text{E UDPGlc} \quad (1)$$

$$\text{E UDPGlc} \rightleftharpoons \text{E}-\text{UMP Glc-1-P} \quad (2)$$

$$\text{E}-\text{UMP Glc-1-P} \rightleftharpoons \text{E}-\text{UMP} + \text{Glc-1-P} \quad (3)$$

valently bonded to His 166. In the uridylylation reactions, the apparent equilibrium constants K^{app} corresponded to eq 4. Under the conditions of the experiments, the concentrations of UDPGlc were saturating, so that [E] ≪ [E UDPGlc], as

$$K^{app} = \frac{\{[\text{E}-\text{UMP}] + [\text{E}-\text{UMP Glc-1-P}]\}[\text{Glc-1-P}]}{\{[\text{E}] + [\text{E UDPGlc}]\}[\text{UDPGlc}]} \quad (4)$$

assured by the value of the dissociation constant for UDPGlc of 0.30 ± 0.07 mM, which had been determined from the kinetics for isotope exchange at equilibrium (*25*). Therefore, the apparent equilibrium constant is given by eq 5, where $[\text{E}-\text{UMP}]_o$ corresponds to the total uridylylated enzyme.

$$K^{app} = \frac{[\text{E}-\text{UMP}]_o[\text{Glc-1-P}]}{[\text{E UDPGlc}][\text{UDPGlc}]} \quad (5)$$

Chemical Modification of C160A-GalT with p-CMB. C160A-GalT was dialyzed against sodium bicinate buffer at pH 8.5 to remove β-mercaptoethanol that had been added during the purification. The dialyzed variant (15 μM) was treated with 200 or 1000 μM *p*-CMB in sodium bicinate buffer. Aliquots were withdrawn at various time intervals, and enzymatic activities were measured using the standard assay. A similar positive control was set up with wild-type enzyme. The measured activities were normalized for the enzyme content added and then plotted as a function of time.

RESULTS

Preparation and Preliminary Assays of C160S-, C160A-, and S161A-GalT. The variants C160S and C160A of GalT were produced by changing the TGC codon for Cys to TCC for Ser and GCC for Ala by use of the Kunkel method for site-directed mutagenesis (*20*). Similarly, the TCT codon for Ser 161 was changed to GCT for Ala to construct the gene expressing S161A-GalT. The resulting mutated genes were overexpressed in *E. coli*. Specific activities of the cell extracts were 14.9 and 9.9 U (mg of protein)$^{-1}$ for C160S- and C160A-GalT, respectively. A similar extract of cells containing the wild-type GalT gene in the same plasmid displayed a specific activity of 16.3 U (mg of protein)$^{-1}$. In contrast, the specific activity of the cell extract from the expression of S161A-GalT was 9.3×10^{-4} U (mg of protein)$^{-1}$. An extract of cells transformed with a similar plasmid that did not contain a wild-type or mutated GalT gene displayed a specific activity of 8.82×10^{-5} U (mg of protein)$^{-1}$ under the same conditions. These results indicated that the mutation of Ser 161 caused GalT to lose most of its catalytic activity. However, the presence of activity above the background activity levels indicated catalysis by the mutated enzyme at a very slow rate.

Table 1: Zinc and Iron Contents of GalT and Point Variants C160A and S161A

	Zn (mol/mol)[a]	Fe (mol/mol)	Zn + Fe (mol/mol)
C160A	1.28 ± 0.03	0.50 ± 0.10	1.78 ± 0.10
S161A	1.18 ± 0.01	0.37 ± 0.10	1.54 ± 0.10
wild type[b]	1.21 ± 0.09	0.67 ± 0.14	1.88 ± 0.14

[a] Moles per mole of enzyme subunits. [b] From ref *10*.

The S161A-GalT, purified as described in Materials and Methods, displayed a specific activity of 2.3×10^{-2} U (mg of protein)$^{-1}$, which is much lower than 180 U (mg of protein)$^{-1}$ observed for wild-type GalT. Therefore, the mutation Ser 161 → Ala 161 caused a 7000-fold loss in GalT activity. In contrast, the purified variant C160A-GalT displayed a specific activity of 79.5 U (mg of protein)$^{-1}$, which is about half the activity of wild-type GalT. Because C160S- and C160A-GalT both displayed similar activities in cell extracts, C160S-GalT was not purified. The activity of C160A-GalT should be representative of the consequences of deleting the thiol group in the active site.

Metal Content of C160A- and S161A-GalT. Ruzicka et al. showed that GalT contained tightly bound zinc and iron (*10*). To test whether the low activity of S161A-GalT might due to a loss of metal ions, we subjected this variant to metal analysis by ICP-MS. The results are shown in Table 1 along with the values for C160A-GalT and wild-type GalT. Both the variants C160A-GalT and S161A-GalT contain the full complement of Zn and Fe, so that the low activity of S161A-GalT cannot be attributed to any loss of metal ions.

Circular Dichroism Spectra of GalT Variants. To assess whether there were major secondary structural differences among the variant and wild-type enzymes, CD spectra were obtained. The spectra of the variant and wild-type enzymes appeared identical (data not shown), indicating similar or identical secondary structures, unlike the zinc-depleted variant H164N-GalT in a recent study, which displayed a major difference in its CD spectrum as compared with wild-type GalT (*27*).

Steady-State Kinetic Parameters for C160A- and S161A-GalT. Steady-state kinetic parameters for C160A-GalT and S161A-GalT were measured at 27 °C with the results shown in Table 2. Kinetic parameters for wild-type and C160A-GalT are similar within a factor of 3. K_m values are somewhat smaller than for the wild-type enzyme, and the value of k_{cat} is similarly smaller, so that the values of k_{cat}/K_m are similar. Somewhat similar results were found for the reaction in the

Table 2: Steady-State Kinetic Parameters for Native and Variant Uridylyltransferases at 27 °C

	WT[a]	C160A	S161A
	Forward Direction		
k_{cat} (s^{-1})	780 ± 19	265 ± 19	(5.4 ± 0.3) × 10^{-2}
K_m^{UDPGlc} (mM)	0.200 ± 0.016	0.082 ± 0.009	0.072 ± 0.007
$K_m^{Gal-1-P}$ (mM)	0.303 ± 0.033	0.125 ± 0.016	0.223 ± 0.017
	Reverse Direction		
k_{cat}(s^{-1})	283 ± 19	55 ± 3	(9.6 ± 0.4) × 10^{-2}
K_m^{UDPGal} (mM)	0.121 ± 0.037	0.078 ± 0.005	0.062 ± 0.004
$K_m^{Glc-1-P}$ (mM)	0.157 ± 0.007	0.138 ± 0.010	0.195 ± 0.011

[a] From ref *23*.

Table 3: First-Order Rate Constants for Uridylyl Transfer by S161A-GalT at 4 °C

	WT[a]	S161A-GalT	WT/ S161A-GalT
uridylylation (UDPGlc) k (s^{-1})	281 ± 18	(3.7 ± 0.02) × 10^{-2}	7.5 × 10^3
de-uridylylation (Glc-1-P) k (s^{-1})	226 ± 10	(1.5 ± 0.02) × 10^{-2}	1.5 × 10^4
de-uridylylation (Gal-1-P) k (s^{-1})	166 ± 13	(0.5 ± 0.05) × 10^{-2}	3.3 × 10^4

[a] From ref *17*.

reverse direction, except that both k_{cat} and k_{cat}/K_m were somewhat smaller than for wild-type GalT.

A striking observation in Table 2 is that the values of k_{cat} are smaller by more than 4 orders of magnitude for S161A-GalT than for wild-type GalT in the forward direction and more than 3 orders of magnitude smaller in the reverse direction. Ser 161 is clearly an important residue supporting catalysis by GalT.

We also measured the steady-state kinetic parameters for S161A-GalT in the forward direction at 4 °C to compare with the single-turnover kinetic parameters, which were available for wild-type GalT at this temperature (*17*). The values of K_m are essentially similar at 4 °C ($K_m^{UDPGlc} = 0.12 \pm 0.01$ and $K_m^{Gal-1-P} = 0.57 \pm 0.04$ mM). The value of k_{cat} is (9.0 ± 0.5) × 10^{-4} s^{-1}. We compared this value of k_{cat} with the rate constants for uridylylation and de-uridylylation at 4 °C (Table 3, and discussed below). The uridylylation rate is 40-fold faster than the overall rate, as expressed by k_{cat}, and the de-uridylylation rate is 5 times faster. These results indicate that de-uridylylation may be slightly more impaired than uridylylation in the case of S161A-GalT. However, neither step is fully rate-limiting.

Uridylylation and De-uridylylation of GalT Variants. We added UDPGlc to the purified C160A-GalT and S161A-GalT at pH 8.5 at 27 °C. C160A-GalT underwent uridylylation rapidly, and the amount of Glc-1-P released showed that all of the active sites in the enzyme were uridylylated. Extended incubation of C160A-GalT with UDPGlc resulted in biphasic kinetics, which was best explained on the basis of the rapid uridylylation of active sites to form the uridylyl-enzyme in the fast phase, followed by the slow hydrolysis of the uridylyl-enzyme to UMP and free enzyme, which reacted further with UDPGlc to release additional Glc-1-P in the slow phase. This phenomenon was also observed in wild-type and other variants of GalT (*17*, *18*). The uridylyl-enzyme form of C160A-GalT can be isolated, and upon reaction with Glc-1-P it produces UDPGlc (data not shown). All uridylylated active sites can undergo the second step of the mechanism rapidly. In essence, C160A behaves similarly to the wild-type enzyme in uridylylation and de-uridylylation.

The variant S161A-GalT underwent 100% uridylylation upon treatment with UDPGlc, but at a much slower rate than GalT or C160A-GalT. S161A-GalT also showed the characteristic biphasic time course for uridylylation (*17*, *18*). Uridylyl-S161A-GalT could be isolated and treated with Glc-1-P to release all bound uridylyl-groups as UDPGlc, again at a slower rate. These results indicate that all the active sites in S161A-GalT remain functional, and that it can undergo uridylylation and de-uridylylation.

The 7000-fold lower activity of S161A-GalT relative to the wild-type enzyme could be correlated with slow uridylylation and de-uridylylation of the mutated enzyme. We measured uridylylation and de-uridylylation rates at 4 °C to compare them with the available uridylylation and de-uridylylation rates for the wild-type enzyme, which were available at 4 °C (*17*). The rate constants were measured under single turnover conditions at saturating concentrations of UDPGlc (uridylylation) or hexose-1-P (de-uridylylation) in the absence of the cosubstrate at 4 °C and compared with published values for the wild-type enzyme. These rate constants are collected in Table 3. Comparison with the transient kinetic uridylylation rate constant of 281 s^{-1} for wild-type enzyme shows that the rate is 7.5 × 10^3 times faster for the wild-type enzyme. The rate difference corresponds to a 4.9 kcal mol^{-1} higher activation energy for the variant S161A-GalT than for the wild-type enzyme. The de-uridylylation rate with Gal-1-P is 3.3 × 10^4-fold slower for S161A-GalT, and this translates to an activation energy difference of 5.7 kcal mol^{-1}. Therefore at 4 °C, both uridylylation of S161A-GalT with UDPGlc and de-uridylylation of its uridylyl-form with Gal-1-P display significantly higher kinetic barriers than the wild-type enzyme.

Equilibrium Energetics of Uridylylation for C160A- and S161A-GalT. Measurement of the equilibrium constant for uridylyl-group transfer to His 166 allows the free energy change associated with the uridylylation reaction to be calculated. We have previously reported values of the equilibrium constant for uridylylation of the wild-type enzyme (*17*). We performed similar measurements on C160A-GalT and S161A-GalT to investigate the effect of the mutations on the thermodynamics of uridylylation. The apparent equilibrium constant (K^{app}) for uridylylation of C160A-GalT measured in triplicate is 0.020 ± 0.008, and the corresponding standard free energy change at pH 8.5 is +2.3 ± 0.9 kcal mol^{-1}. The equilibrium constant for uridylylation of S161A-GalT measured in triplicate is 0.022 ± 0.002, corresponding to a standard free energy change at pH 8.5 of +2.3 ± 0.2 kcal mol^{-1}. The equilibrium constant reported for uridylylation of wild-type GalT is 0.005 ± 0.002, corresponding to a standard free energy change of +3.2 kcal mol^{-1} (*17*). These results indicate that the side chain of neither Cys 160 nor Ser 161 provides stabilization for the uridylyl-enzyme at equilibrium. We previously observed a similar behavior in the case of the Gln 168 variants and concluded that Gln 168 was not involved in stabilizing the uridylyl-enzyme intermediate (*17*). In fact, the absence of the side chains of Cys 160, Ser 161, or Gln 168 increases the value of K^{app}, which indicates apparent stabilization of the uridylyl-enzyme in these variants. Examination of eqs

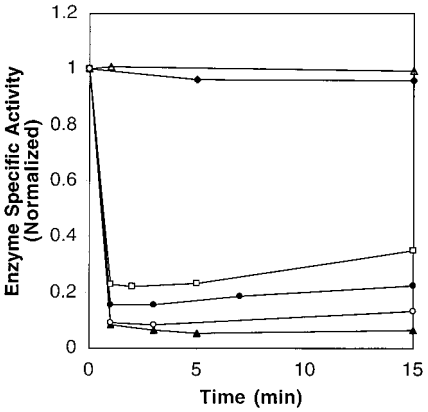

FIGURE 2: Chemical modification of C160A-GalT with *p*-CMB. C160A enzyme was dialyzed against sodium bicinate buffer at pH 8.5 to remove β-mercaptoethanol that had been added as a reductant during the purification. Thiol-free variant enzyme (15 μM) was treated with 0 (open triangles), 200 (closed circles), or 1000 μM (open circles) *p*-CMB in sodium bicinate buffer. Aliquots were taken at various time intervals, and the activity of the enzyme was measured using the standard assay. A similar positive control was set up with wild-type enzyme with 0 (closed diamonds), 200 (open squares), or 1000 μM (closed triangles) *p*-CMB. Measured activities were normalized 100% activity at time zero, and the residual activities were plotted as a function of time. Results show that both wild-type and C160A-GalT are inactivated by *p*-CMB.

3−5 indicates that stabilization may arise either from more favorable binding interactions between the mutated forms of GalT and the UMP-moiety of E−UMP or from stronger binding of Glc-1-P to the mutated forms of E−UMP.

Chemical Modification of C160A-GalT with p-CMB. Early results indicated a sensitivity of GalT toward reagents that selectively modify cysteine residues (*19*). GalT loses its activity when treated with the cysteine modifying reagent *p*-CMB. Because Cys 160 was found in the active site, it seemed that its chemical modification might cause a loss of enzyme activity. We carried out chemical modification of wild-type and C160A-GalT with *p*-CMB, with the results shown in Figure 2. Wild-type GalT was inactivated by 0.2 or 1.0 mM *p*-CMB within 1 min, and the enzyme remained inactive for longer than 15 min. The control experiment in which *p*-CMB was excluded showed no activity loss. If Cys 160 were the residue whose modification inactivated GalT, then similar treatment with *p*-CMB would not cause C160A-GalT to lose activity. However, the C160A variant showed activity losses similar to wild-type enzyme at 0.2 and 1.0 mM *p*-CMB levels. These results allow us to conclude that inactivation by *p*-CMB cannot be attributed to the chemical modification of Cys 160. An alternative scenario is that chemical modification of either Cys 160 or one or more of the other five cysteine residues can inactivate the enzyme. In this case, chemical modification of Cys 160 would inactivate the wild-type enzyme by blocking the active site; however, in C160A-GalT, no reaction occurs in the active site, and Cys 160 is not required for activity. Inactivation of C160A-GalT by *p*-CMB would result from chemical modification at other sites.

DISCUSSION

GalT catalyzes nucleotidyl transfer with the formation of a high-energy uridylyl-enzyme intermediate. It is known that His 166, which is transiently nucleotidylated at $N^{\epsilon 2}$, retains the proton at $N^{\delta 1}$ (*18*). Therefore, inasmuch as the apparent pK_a for the imidazolyl group is elevated by at least 3.3 units, the uridylyl-enzyme must be stabilized by noncovalent interactions by at least 4.5 kcal mol^{-1}. The transition states for uridylylation and de-uridylylation should be stabilized for efficient catalysis. Gln 168, Cys 160, and Ser 161 seemed to be likely candidates to provide such stabilization of the transition states and intermediate. It had been found, however, that Gln 168 did not stabilize the uridylyl-enzyme intermediate and that Q168N and Q168G variants retained significant enzymatic activity (*17*). Therefore, we focused attention on Cys 160 and Ser 161 and investigations of their roles in uridylyl-enzyme stabilization and transition-state stabilization.

The present results show that neither Cys 160 nor Ser 161 stabilizes the uridylyl-enzyme intermediate in terms of the free energy of uridylyl-group transfer. If the uridylyl-enzyme had been stabilized, the standard free energy for uridylylation of C160A- and S161A-GalT would be less favorable than for wild-type GalT. However, the free energies for uridylylation of these two intermediates are more favorable (less positive) than in the case of wild-type GalT. A simple rationale for this observation is that the loss of the respective side chains makes other noncovalent interactions stronger in the uridylyl-enzyme intermediate, thereby lending an apparent minor stabilization to the intermediate. Alternatively, Ser 161 and Cys 160 may slightly destabilize the uridylyl-enzyme relative to the free enzyme.

Kinetic studies on C160A-GalT and S161A-GalT show that S161A-, but not C160A-GalT, is significantly less active than wild-type GalT. S161A-GalT behaves similarly to wild-type GalT during purification, it displays the same metal content, all the active sites are functional (100% uridylylation and de-uridylylation), and the steady-state kinetic parameters are similar to wild-type values except for k_{cat}, which is much smaller ($10^{-4}\times$ wild type). Therefore the loss of activity is strictly a kinetic phenomenon.

Our measurement of uridylylation and de-uridylylation rates for S161A-GalT shows that both steps in the mechanism are affected. The higher kinetic barriers for individual steps result in a 7000-fold loss in overall turnover for the variant enzyme. In the crystal structure of the complex of H166G-GalT with UDPGlc, Ser 161 is only 2.6 Å from the β-phosphoryl oxygens. Ser 161 may be involved in donating a hydrogen bond to a β-phosphoryl oxygen in the ternary complex and during the transition states for uridylylation and de-uridylylation. The main chain amide hydrogen of Ser 161 also forms a hydrogen bond to an α-phosphoryl oxygen. Therefore, it is likely that Ser 161 is involved in correctly positioning the α- and β-phosphate groups, such that His 166 $N^{\epsilon 2}$ is aligned with the α-phosphorus and poised for nucleophilic attack. Chemically, the donation of a proton to Glc-1-P does not facilitate the reaction. However, the donation of a hydrogen bond to the β-phosphoryl group could fix it in position for optimal nucleophilic attack. The hydrogen bond between the Ser 161 main chain amide and the α-phosphoryl oxygen may provide stabilization to the transition state.

Once the uridylyl-enzyme is formed, Ser 161 rotates approximately 90° away from the active site (*12*, *14*). When the hexose-1-phosphate acceptor binds to the uridylyl-enzyme for the second step, Ser 161 probably rotates back toward

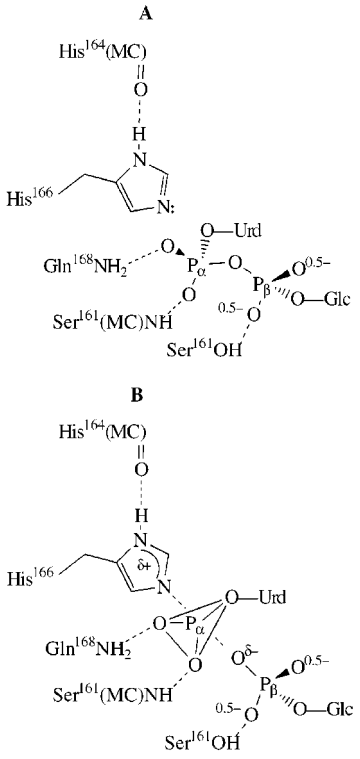

FIGURE 3: Schematic diagram interactions in a Michaelis complex and the transition state for uridylyl-transfer by GalT. (A) UDPGlc bound at the active site is oriented for nucleophilic attack by hydrogen bonds between phosphoryl oxygens and Ser 161 side chain (β-phosphoryl), Ser 161 main chain (MC) NH (α-phosphoryl), and Gln 168 (α-phosphoryl). (B) In the transition state, a β-phosphoryl oxygen is properly oriented by hydrogen bonding with the side chain of Ser 161. The side chain of Gln 168 and the main chain NH of Ser 161 attenuates the build-up of negative charge, thereby stabilizing the transition state. The imidazole ring of His 166 ring acquires positive charge in the transition state, and the $N^{\delta 1}$ proton is held in place by an interaction with the backbone carbonyl group of His 164.

the substrate and donates a hydrogen bond to the hexose-1-phosphate oxygen. This probably guides and orients the phosphoryl group to attack the uridylyl-enzyme. On the basis of these results, we have proposed a model for GalT catalysis (Figure 3), in which Gln 168 and Ser 161 donate hydrogen bonds to the α- and β-phosphoryl oxygen atoms, respectively, in the transition state for uridylyl-group transfer.

The rotation of Ser 161 away from the active site results in Cys 160 being rotated toward the α-phosphoryl group and apparently forming a hydrogen bond (*12*). However, the presence of cysteine in this position is not critical for activity, and our results show that either Ser or Ala at this position supports catalysis equally. The overall k_{cat} in the forward direction for C160A is 265 s^{-1} at 27 °C, and this is only 3-fold slower than the wild-type enzyme. Rate constants for uridylylation and de-uridylylation have to be faster than 265 s^{-1}, and it is unlikely that either step has been slowed significantly as compared to wild-type values. The K_m values for C160A remain essentially the same as for wild-type GalT. It has been hypothesized that having a Cys interacting with the uridylyl-enzyme provided a weak hydrogen bond to stabilize the uridylyl-enzyme while preventing nonproductive hydrolysis of the uridylyl-enzyme (*12*). But, the high activities of C160S- and C160A-GalT suggest that such hydrolysis, even if it occurs, is catalytically insignificant. Chemical modification studies show that Cys 160 is unlikely to be the residue modified by *p*-CMB that inactivates the wild-type enzyme. Therefore, despite being highly conserved and showing an interaction with the uridylyl-group in the crystal structure, Cys 160 does not make a significant contribution to catalysis.

Our results leave a few more questions about GalT unanswered. While we have been successful in identifying a residue that is involved in transition-state stabilization and substrate orientation, it is still unclear how the uridylyl-enzyme is stabilized. Even though the protonated His 166 N^{δ} has a direct interaction with the backbone carbonyl oxygen of His 164, it is unlikely that this alone can account for the stabilization. We have shown in this and previous work that three residues directly interacting with phosphoryl oxygens do not contribute to uridylyl-enzyme stabilization. Therefore, this stabilization must occur by interactions at the other portions of the substrate. Asp 78, Asn 77, and Val 61 interact with the uridine portion and may play a role in uridylyl-enzyme stabilization by hydrogen bond donation and hydrophobic interactions.

ACKNOWLEDGMENT

We thank Adrian D. Hegeman for providing UDPGal-4-epimerase and Dr. Darrell McCaslin for help in obtaining CD spectra. All kinetic data were fitted by the use of programs written by Dr. W. W. Cleland, and the authors are grateful to him for his generosity in providing programs for our use.

REFERENCES

1. Leloir, L. F. (1971) *Science 172*, 1299−1303.
2. Hill, H. Z., and Puck, T. T. (1973) *Science 179*, 1136−1139.
3. Segal, S. (1989) *The Metabolic Basis of Inherited Disease*, 6th ed., McGraw-Hill, New York.
4. Podskarbi, T., Reichardt, J., and Shin, Y. S. (1994) *J. Inherited Metab. Dis. 17*, 149−150.
5. Cramer, D. W., Harlow, B. L., Barbieri, R. L., and Ng, W. G. (1989) *Fertil. Steril. 51*, 609−615.
6. Kaufman, F. R., Devgan, S. D., and Donnell, G. N. (1993) *Fertil. Steril. 60*, 727−728.
7. Fridovich-Keil, J. L., and Jinks-Robertson, S. (1993) *Proc. Natl. Acad. Sci. U.S.A. 90*, 398−402.
8. Lemaire, H. G., and Mueller-Hill, B. (1986) *Nucleic Acids Res. 14*, 7705−7711.
9. Cornwell, T. L., Adhya, S. L., Reznikoff, W. S., and Frey, P. A. (1987) *Nucleic Acids Res. 15*, 8116.
10. Ruzicka, F. J., Wedekind, J. E., Kim, J., Rayment, I., and Frey, P. A. (1995) *Biochemistry 34*, 5610−5617.
11. Wedekind, J. E., Frey, P. A., and Rayment, I. (1995) *Biochemistry 34*, 11049−11061.
12. Wedekind, J. E., Frey, P. A., and Rayment, I. (1996) *Biochemistry 35*, 11560−11569.
13. Kim, J., Ruzicka, F. J., and Frey, P. A. (1990) *Biochemistry 29*, 10590−10593.
14. Thoden, J. B., Ruzicka, F. J., Frey, P. A., Rayment, I., and Holden, H. M. (1997) *Biochemistry 36*, 1212−1222.
15. Elsas, L. J., Fridovich-Keil, J. L., and Leslie, N. D. (1993) *Int. Pediatr. 8*, 101−109.
16. Ng, W. G., Xu, Y. K., Kaufman, F. R., Donnell, G. N., Wolff, J., Allen, R. J., Koritala, S., and Reichardt, J. K. V. (1994) *Hum. Genet. 94*, 359−363.
17. Geeganage, S., and Frey, P. A. (1998) *Biochemistry 37*, 14500−14507.
18. Ruzicka, F. J., Geeganage, S., and Frey, P. A. (1998) *Biochemistry 37*, 11385−11392.

19. Wong, L.-J., Sheu, K.-F., Lee, S.-L., and Frey, P. A. (1977) *Biochemistry 16*, 1010−1016.
20. Kunkel, T. A. (1985) *Proc. Natl. Acad. Sci. U.S.A. 82*, 488−492.
21. Wedekind, J. E., Frey, P. A., and Rayment, I. (1994) *Acta Crystallogr. D50*, 329−331.
22. Arabshahi, A., Ruzicka, F. J., Geeganage, S., and Frey, P. A. (1996) *Biochemistry 35*, 3426−3428.
23. Wong, L.-J., and Frey, P. A. (1974) *Biochemistry 13*, 3889−3894.
24. Cleland, W. W. (1979) *Methods Enzymol. 63*, 103−138.
25. Wong, L.-J. (1974) Ph.D. Dissertation, The Ohio State University.
26. Smith, T. J. (1995) *J. Mol. Graphics 13*, 122−125.
27. Geeganage, S., and Frey, P. A. (1999) *Biochemistry 38*, 13398−13406.

BI992594S